

## QUADRUPOLE DEFORMATION OF $^{110}\text{Cd}$ STUDIED WITH COULOMB EXCITATION\*

K. WRZOSEK-LIPSKA<sup>a</sup>, L. PRÓCHNIAK<sup>a</sup>, P.E. GARRETT<sup>b</sup>  
 S.W. YATES<sup>c,d</sup>, J.L. WOOD<sup>e</sup>, P.J. NAPIORKOWSKI<sup>a</sup>, T. ABRAHAM<sup>a</sup>  
 J.M. ALLMOND<sup>f</sup>, F.L. BELLO GARROTE<sup>g</sup>, H. BIDAMAN<sup>b</sup>  
 V. BILDSTEIN<sup>b</sup>, C. BURBADGE<sup>b</sup>, M. CHIARI<sup>h</sup>, A. DIAZ VARELA<sup>b</sup>  
 D.T. DOHERTY<sup>i,j</sup>, S. DUTT<sup>k</sup>, K. HADYŃSKA-KŁĘK<sup>a,g</sup>, M. HLEBOWICZ<sup>l</sup>  
 J. IWANICKI<sup>a</sup>, B. JIGMEDDORJ<sup>b</sup>, M. KISIELIŃSKI<sup>a</sup>, M. KOMOROWSKA<sup>a</sup>  
 M. KOWALCZYK<sup>a</sup>, R. KUMAR<sup>m</sup>, T. MARCHLEWSKI<sup>a</sup>  
 M. MATEJSKA-MINDA<sup>a,n</sup>, B. OLAIZOLA<sup>b</sup>, F. OLESZCZUK<sup>l</sup>, M. PALACZ<sup>a</sup>  
 E. PASQUALI<sup>o</sup>, E.E. PETERS<sup>d</sup>, M. ROCCHINI<sup>b,p</sup>, E. SAHIN<sup>g</sup>  
 M. SAXENA<sup>q</sup>, J. SREBRNY<sup>a</sup>, A. TUCHOLSKI<sup>a</sup>

<sup>a</sup>Heavy Ion Laboratory, University of Warsaw, Poland

<sup>b</sup>University of Guelph, Ontario, Canada

<sup>c</sup>Dept. of Physics and Astronomy, University of Kentucky, Lexington, KY, USA

<sup>d</sup>Dept. of Chemistry, University of Kentucky, Lexington, KY, USA

<sup>e</sup>School of Physics, Georgia Institute of Technology, Atlanta, Georgia, USA

<sup>f</sup>Physics Division, Oak Ridge National Laboratory, USA

<sup>g</sup>Dept. of Physics, University of Oslo, Norway

<sup>h</sup>INFN e Università di Firenze, Italy

<sup>i</sup>University of Surrey, Guildford, UK

<sup>j</sup>IRFU/DPhN, CEA, Université Paris-Saclay, Gif-sur-Yvette, France

<sup>k</sup>Dept. of Physics, Aligarh Muslim University, India

<sup>l</sup>Faculty of Physics, Warsaw University of Technology, Poland

<sup>m</sup>Inter University Accelerator Centre, New Delhi, India

<sup>n</sup>Institute of Nuclear Physics Polish Academy of Sciences, Kraków, Poland

<sup>o</sup>Università di Camerino, Italy

<sup>p</sup>INFN Sezione di Firenze, Italy

<sup>q</sup>Dept. of Physics and Astrophysics, University of Delhi, New Delhi, India

*(Received December 11, 2019)*

The low-energy electromagnetic structure of  $^{110}\text{Cd}$  was studied using safe-energy Coulomb excitation at the Heavy Ion Laboratory, University of Warsaw. The preliminary results on the quadrupole deformation of low-lying  $0^+$  states in  $^{110}\text{Cd}$  are presented and compared to the recent beyond-mean-field and General Bohr Hamiltonian calculations.

DOI:10.5506/APhysPolB.51.789

---

\* Presented at the XXXVI Mazurian Lakes Conference on Physics, Piaski, Poland, September 1–7, 2019.

## 1. Introduction

The stable even–even Cd isotopes have played a pivotal role in the investigation of collective behavior in nuclei for over 40 years. Early work suggested that the even-mass Cd isotopes near the mid-neutron shell were textbook examples of near-harmonic vibrational behavior. This widespread belief was based on the observed pattern of low-lying excited states in the Cd isotopes. This perspective was, however, complicated by large values of the quadrupole moments of the  $2_{1,2}^+$ ,  $4_1^+$  and  $6_1^+$  states in  $^{114}\text{Cd}$  [1] and the appearance of low-lying shape-coexisting intruder states in  $^{110}\text{Cd}$  [2]. The well-established view that the Cd isotopes behave as vibrational nuclei underwent a rather rapid shift in the last 20 years as a result of comprehensive spectroscopy of the  $^{110,112,114,116}\text{Cd}$  nuclei using the  $(n, n'\gamma)$  reaction [3–6], as well as highly sensitive  $\beta$ -decay studies [4, 7] and g-factor measurements [8]. These experimental findings lead to the fundamental question regarding the nature of collectivity of the low-lying states in Cd nuclei (see, *e.g.*, Refs. [9, 10]), particularly the first excited  $0^+$  states, which were invariably interpreted as multi-phonon structures. With the present knowledge of spectroscopic data, shape coexistence need to be invoked to account for their character. Indeed, very recent results of beyond-mean-field calculations suggest that each of the first four  $0^+$  states in  $^{110,112}\text{Cd}$  presents a different quadrupole shape [11, 12].

Nowadays, the most critical needs are to establish the underlying structures of low-lying  $0^+$  states, particularly for  $^{110,112}\text{Cd}$ , to validate the shape-coexistence scenario and to reveal whether or not the Cd isotopes possess multi-phonon  $0^+$  excited states. Multi-step Coulomb excitation can provide essential data to advance our understanding of the nature of such low-energy states. However, detailed Coulomb-excitation studies of stable cadmium isotopes are surprisingly scarce and, so far, have only been performed for  $^{114}\text{Cd}$  [1]. Coulomb-excitation experiments for other stable Cd isotopes were generally limited to single-step studies performed in the early 1960s and 1970s with beams of protons,  $\alpha$  particles and  $^{16}\text{O}$  ions (*e.g.* Refs. [13, 14]).

## 2. Coulomb excitation of $^{110}\text{Cd}$

A Coulomb-excitation experiment to study  $^{110}\text{Cd}$  was performed at the Heavy Ion Laboratory, University of Warsaw, using a 91 MeV  $^{32}\text{S}$  beam delivered by the Warsaw cyclotron. The  $\gamma$  rays emitted from the Coulomb-excited states were detected by 15 Compton-suppressed HPGe detectors of 25%–30% efficiency relative to a  $3\times 3$  inch NaI detector, forming the EAGLE  $\gamma$ -ray spectrometer [15]. An array of 48 PIN-diode detectors [16, 17] was used to register back-scattered  $^{32}\text{S}$  ions in coincidence with detected  $\gamma$  rays. The particle detectors covered the laboratory angular range from  $119^\circ$  to  $168^\circ$ , which corresponds to centre-of-mass angles from  $134^\circ$  to  $171^\circ$ . An enriched (97.36%)  $^{110}\text{Cd}$  target of  $1.3\text{ mg/cm}^2$  thickness was used.



Several states in  $^{110}\text{Cd}$  were populated with sufficient cross section to be observed in the present experiment, predominantly through one- and two-step Coulomb-excitation processes. In addition to the ground-state band, low-lying, non-yrast levels were also excited. The  $0_2^+$ ,  $2_2^+$ ,  $4_1^+$  states of similar energies, often interpreted within the vibrational model as belonging to the two-phonon triplet, are strongly populated, while the  $0_3^+$  state was at the observational limit. A peak around 816 keV is identified as a doublet of the  $2_2^+ \rightarrow 2_1^+$  and  $0_2^+ \rightarrow 2_1^+$   $\gamma$ -ray transitions at energies of 818 keV and 815 keV, respectively. A contribution from the  $2_2^+ \rightarrow 2_1^+$  transition can be determined using the measured intensity of the  $2_2^+ \rightarrow 0_1^+$   $\gamma$ -ray transition at 1476 keV and the well-known  $\gamma$ -ray branching ratios for transitions de-exciting the  $2_2^+$  state. The remaining intensity of the 816-keV doublet transitions was attributed to the  $0_2^+ \rightarrow 2_1^+$ .

It is worth noting that no transitions from the  $0_{2,3}^+$  states were observed in the earlier Coulomb-excitation measurements performed with beams of protons, alpha particles or  $^{16}\text{O}$  ions [13, 14]. The data analysis is on-going aiming at extraction of a complete set of electromagnetic matrix elements between low-lying states of  $^{110}\text{Cd}$  populated in the experiment.

### 3. Quadrupole deformation of the $0_1^+$ and $0_2^+$ states in $^{110}\text{Cd}$ — experimental findings

Within the Cline–Kumar sum rule approach [19, 20], quadrupole shape invariants are constructed, which provide a relationship between the charge distribution of the nucleus in a given nuclear state and the reduced E2 matrix elements. The nuclear charge distribution is described using two parameters,  $Q$  and  $\delta$ , which are analogous to and can be related to Bohr's  $\beta$  and  $\gamma$  parameters [23]. However, the latter correspond to the mass, rather than the charge distribution. The simplest quadrupole invariant,  $\langle Q^2 \rangle$ , describes the overall deformation, while the information on non-axiality can be obtained from the  $\langle Q^3 \cos(3\delta) \rangle$  invariant. For an integral-spin system, the two lowest-order invariants are

$$\langle Q^2 \rangle = \frac{\sqrt{5}}{\sqrt{(2I_i + 1)}} \sum_t \langle i \| E2 \| t \rangle \langle t \| E2 \| i \rangle \left\{ \begin{matrix} 2 & 2 & 0 \\ I_i & I_t & I_t \end{matrix} \right\}, \quad (1)$$

$$\langle Q^3 \cos(3\delta) \rangle = \sqrt{\frac{35}{2}} \frac{-1}{(2I_i + 1)} \sum_{t,u} \langle i \| E2 \| u \rangle \langle u \| E2 \| t \rangle \langle t \| E2 \| i \rangle \left\{ \begin{matrix} 2 & 2 & 2 \\ I_i & I_t & I_u \end{matrix} \right\}. \quad (2)$$

This method, independent of nuclear models, is particularly useful for attributing shape parameters to low-lying  $0^+$  states as demonstrated, for example, in Refs. [21–23]. In such cases only matrix elements involving  $0^+$  and  $2^+$  states enter the sums in Eqs. (1) and (2). While the  $\langle Q^2 \rangle$  invariant for the ground state in even–even nuclei is dominated by the contribution

from the  $\langle 0_1^+ || E2 || 2_1^+ \rangle$  matrix element (see, *e.g.*, Ref. [23]), the situation is more complex for the higher-order invariants, *e.g.*,  $\langle Q^3 \cos(3\delta) \rangle$ , since in these cases knowledge of the relative signs of the transitional E2 matrix elements as well as of the quadrupole moments of excited  $2^+$  states becomes crucial.

Preliminary values of reduced E2 matrix elements obtained in the present study permit some conclusions to be reached on the quadrupole deformation of  $^{110}\text{Cd}$  in its ground and first excited  $0^+$  states. A similar overall deformation is found for the  $0_1^+$  and  $0_2^+$  states of  $^{110}\text{Cd}$ , as indicated by the  $\langle Q^2 \rangle$  values of  $0.44(1) e^2 b^2$  ( $\langle \beta^2 \rangle^{1/2} \approx 0.17$ ) and  $0.51(8) e^2 b^2$  ( $\langle \beta^2 \rangle^{1/2} \approx 0.19$ ), respectively. The  $\langle \cos(3\delta) \rangle$  value for the  $0_1^+$  ground state was estimated to be  $0.35(5)$ , which corresponds to the non-axiality parameter  $\langle \delta \rangle \approx \langle \gamma \rangle \approx 23^\circ$ . The lack of experimental information on key matrix elements, particularly  $\langle 2_3^+ || E2 || 2_3^+ \rangle$ , prevents us from drawing firm conclusions on the nature of the deformation of the  $0_2^+$  state, as discussed further in Section 5.

#### 4. Quadrupole deformation of $^{110}\text{Cd}$ from the recent mean-field theories

The structure of the stable even–even Cd nuclei was recently investigated using various theoretical approaches based on the interacting-boson model (IBM) [24, 25] or mean-field descriptions [11, 12]. In particular, the results of the recent beyond-mean-field (BMF) calculations [11, 12], employing the symmetry conserving configuration mixing method with the Gogny D1S energy density functional, suggest that the Cd isotopes exhibit multiple shape coexistence, *i.e.*, different and unique quadrupole shapes were predicted for the first four  $0^+$  states in  $^{110}\text{Cd}$  and  $^{112}\text{Cd}$ . These theoretical findings are consistent with those of self-consistent calculations performed with the General Bohr Hamiltonian (GBH) model presented in this section. These calculations are an extension of the previous work published in Ref. [26].

A general introduction to the GBH approach can be found in Ref. [27], while the recent examples of its application to Mo and Xe isotopes are presented in Refs. [23, 28]. The GBH is determined by seven functions: six inertial functions and the potential energy. These functions are obtained from the microscopic mean-field theory using the adiabatic time-dependent Hartree–Fock–Bogoliubov (ATDHFB) approach and employing effective nucleon–nucleon interactions of the Skyrme type. In the present work, two distinct Skyrme-type effective microscopic interactions were used: SLy4, and the more recent UNEDF0. The HFB calculations are performed in the space of dynamical variables of the model, *i.e.*, including the full  $\beta$ – $\gamma$  plane. At the final stage, the eigenequation for the GBH is solved yielding the level energies and the collective wave functions, which are used to compute the electromagnetic properties of the nucleus, *e.g.*, transitional and

diagonal E2 matrix elements. The GBH model treats simultaneously and on equal footing both vibrational and rotational excitations, and describes the full quadrupole dynamics including both of these degrees of freedom.

The probability density distributions in the  $\beta$ - $\gamma$  plane determined by the eigenfunctions of the Bohr Hamiltonian are presented in Fig. 3 for the three lowest-lying  $0^+$  states in  $^{110}\text{Cd}$ . The results obtained for the excited  $0_2^+$  and  $0_3^+$  states clearly differ depending on the interaction (SLy4 or UNEDF0) used in the calculations, while that seems not to be the case for the  $0_1^+$  ground state (see Fig. 3). The GBH (UNEDF0) calculations suggest a similar magnitude of the overall deformation for all considered  $0^+$  states with their probability density distributions being widely spread in the  $\gamma$  parameter and resembling those obtained for a harmonic oscillator potential. The results obtained with the SLy4 interaction are considerably different, indicating that the first three  $0^+$  states are characterized by various types of deformation. According to these calculations,  $^{110}\text{Cd}$  undergoes a transition from a considerably triaxial, moderately deformed shape ( $\beta \approx 0.2$ ,  $\gamma \approx 22^\circ$ ) in the ground state, through a more deformed ( $\beta \approx 0.3$ ) prolate one in the  $0_2^+$  state, towards a more oblate deformation in the  $0_3^+$  state. This scenario closely resembles that predicted by the BMF calculations of Refs. [11, 12].

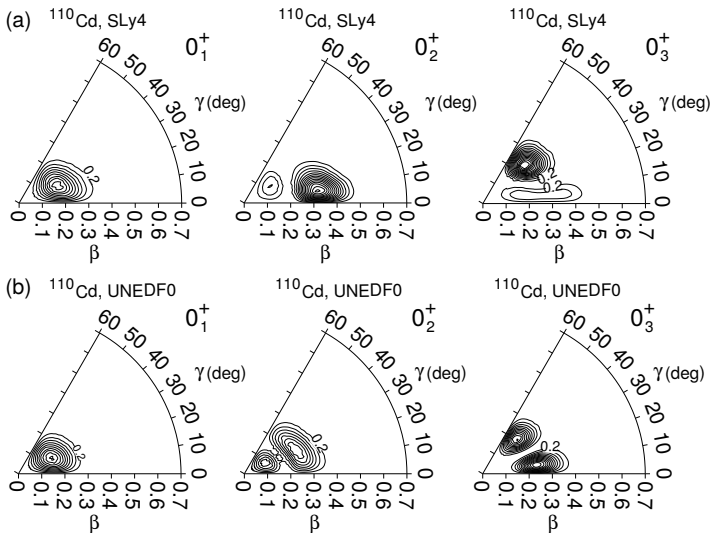


Fig. 3. Probability density distributions for the  $0_1^+$ ,  $0_2^+$  and  $0_3^+$  states in  $^{110}\text{Cd}$  calculated within the GBH approach using Skyrme SLy4 (a) and UNEDF0 (b) interactions.

The GBH model predictions for the deformation of the  $0^+$  ground state of  $^{110}\text{Cd}$ , including its non-axiality, reproduce well the experimental findings reported in Section 3. However, the overall deformation of the  $0_2^+$  state is

overestimated by GBH (SLy4) by a factor of  $\sim 1.5$ . The use of the UNEDF0 parametrization in GBH calculations yields a slightly lower deformation for the  $0_2^+$  state, which is more consistent with the experimental result.

## 5. Outlook

The possibility that the Cd isotopes present multiple coexisting shapes clearly demands further investigation. The well-established Coulomb-excitation technique represents an ideal tool to study nuclear shapes as presented in Section 3. However, in order to confirm that the lowest-lying  $0^+$  states are indeed characterized by different quadrupole deformations, much richer and more detailed experimental information is required. In particular, precise knowledge of the E2 matrix elements involving several excited  $0^+$  and  $2^+$  states, including their relative signs, as well as quadrupole moments ( $Q_{sp}$ ) of the excited  $2^+$  states, is required. In order to establish a value for the non-axiality parameter for the  $0_2^+$  state, information on the  $Q_{sp}(2_3^+)$  value is crucial, as shown in Fig. 4. From the same plot, it is clear that the contribution from the unknown relative signs of the  $\langle 2_3^+ || E2 || 2_2^+ \rangle$ ,  $\langle 2_3^+ || E2 || 2_1^+ \rangle$  and  $\langle 2_3^+ || E2 || 0_2^+ \rangle$  matrix elements is minor. A possible impact of couplings with the  $2_{4,5}^+$  states was estimated to be negligible based on the relevant E2 matrix elements calculated within the GBH approach.

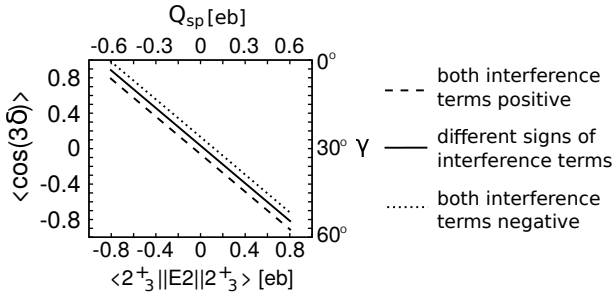


Fig. 4. Non-axiality parameter for the  $0_2^+$  state in  $^{110}\text{Cd}$  calculated as a function of the quadrupole moment of the  $2_3^+$  state. The dashed, dotted and solid lines correspond to different combinations of signs of the interference terms:  $\langle 0_2^+ || E2 || 2_1^+ \rangle \langle 2_1^+ || E2 || 2_3^+ \rangle \langle 2_3^+ || E2 || 0_2^+ \rangle$  and  $\langle 0_2^+ || E2 || 2_2^+ \rangle \langle 2_2^+ || E2 || 2_3^+ \rangle \langle 2_3^+ || E2 || 0_2^+ \rangle$ . The calculations were performed using experimentally known E2 matrix elements determined from the measurement presented in this work and in Ref. [6].

To extract the deformation of the  $0_3^+$  state, the  $B(E2; 0_3^+ \rightarrow 2_{1,2}^+)$  values need to be precisely measured, while currently only their upper limits are known [6]. Drawing firm conclusions about the non-axiality parameter for the  $0_3^+$  state in  $^{110}\text{Cd}$  is much more complex as a significantly larger set of matrix elements contributes to this value. In addition to the already measured E2 matrix elements coupling the  $2_1^+$ ,  $2_2^+$  and  $2_3^+$  states, those between

the  $0_3^+$  and  $2_{2,3,4}^+$  states need to be known, as well as the  $\langle 2_4^+ || E2 || 2_{2,3}^+ \rangle$  elements together with their relative signs. Moreover, the quadrupole moments of the  $2_{4,5}^+$  states may play an important role as well. Again, the impact of unknown matrix elements may be estimated using their values predicted by the GBH model.

In order to extract the aforementioned matrix elements, which are crucial to determine the shape parameters of the excited  $0^+$  states in  $^{110}\text{Cd}$ , a series of systematic Coulomb-excitation experiments needs to be performed. Coulomb-excitation cross sections depend on beam energy, scattering angle as well as the atomic ( $Z$ ) and mass ( $A$ ) numbers of the beam and target nuclei. With the use of high- $Z$  reaction partners, the excitation is no longer limited to single transitions from the ground state. Instead, a large number of states can be accessed via multi-step excitation. In such cases, a number of matrix elements affects the Coulomb-excitation cross section in a complex way, with the contribution from various excitation paths varying with the scattering angle. It is possible to disentangle them from differential measurements of Coulomb-excitation cross sections, gaining sensitivity to subtle higher-order effects, such as spectroscopic quadrupole moments and relative signs of matrix elements [29]. Moreover, measurements with reaction partners of lower  $Z$  (*i.e.*,  $^{58}\text{Ni}$  or  $^{32}\text{S}$  beams on Cd targets) are needed to assist in elucidating the various excitation paths and determining the electromagnetic structure of the low-energy part of the level scheme.

The expected population of low-lying yrast and non-yrast excited states in  $^{110}\text{Cd}$  for various beam–target combinations is presented in Fig. 5. The calculations were performed with the GOSIA code [30, 31] assuming the

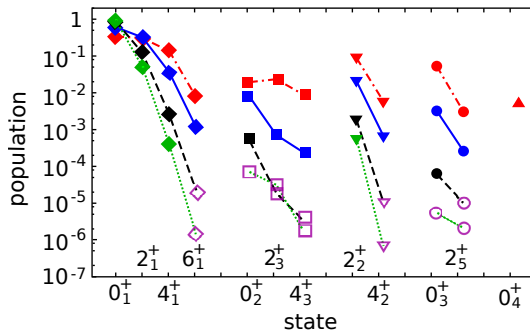


Fig. 5. (Color online) Estimated cross sections for populating the low-lying yrast and non-yrast states in  $^{110}\text{Cd}$  using Coulomb excitation by various reaction partners:  $^{12}\text{C}$  (dotted green line),  $^{32}\text{S}$  (dashed black line),  $^{58}\text{Ni}$  (solid blue line) and  $^{208}\text{Pb}$  (dash-dotted red line). The levels are grouped into bands according to the results of Refs. [10, 11]. For the  $^{12}\text{C}$  and  $^{32}\text{S}$  beams, most higher-lying yrast and non-yrast states are below the observation limit and are marked with open, purple symbols.



known values of matrix elements [6, 18]. One can observe that the Coulomb-excitation cross sections for populating the higher-lying states, *e.g.*,  $4_{1,2,3}^+$ ,  $6_1^+$  or  $0_{2,3}^+$ , which requires a three- or two-step excitation process, are lower by one or two orders of magnitude with respect to the one-step excitation of, *e.g.*, the  $2_1^+$  state. Furthermore, for light-ion beams, *i.e.*,  $^{12}\text{C}$ , the excitation pattern is dominated by single-step excitations (*e.g.*,  $2_1^+$  and  $2_2^+$ ), which limits the number of states that can be observed in such studies. The two-step excitation process is, in such a case, strongly hindered and only the population of the  $4_1^+$  state in the ground-state band can be observed. The cross sections for the two-, three- or more-step excitations are clearly enhanced when using higher- $Z$  reaction partners, *i.e.*,  $^{32}\text{S}$  ( $Z = 16$ ),  $^{58}\text{Ni}$  ( $Z = 28$ ) and  $^{208}\text{Pb}$  ( $Z = 82$ ). Systematic Coulomb-excitation studies of the stable even-even Cd isotopes are planned for the near future. In particular, measurements at the LNL Legnaro facility are considered, with the use of the high-efficiency GALILEO (or AGATA) germanium array coupled with the SPIDER segmented silicon detector [32]. The stable Cd beams will be Coulomb excited on targets with high atomic number, *e.g.*,  $^{208}\text{Pb}$ , in order to maximize the probability of multi-step excitations. These studies will be complemented by experiments with lower- $Z$  beams (*e.g.*  $^{32}\text{S}$  or  $^{58}\text{Ni}$  on a Cd target) at the Heavy Ion Laboratory. Such a combination of experimental efforts will help in disentangling the contributions of numerous electromagnetic matrix elements involved in the excitation process and, consequently, allow the determination of the quadrupole shape parameters of the low-lying  $0^+$  states in the stable Cd nuclei, thus presenting a stringent test of the shape-coexistence scenario predicted by state-of-the-art theoretical calculations.

We acknowledge support from the National Science Centre, Poland (NCN) under grant No. 2013/10/M/ST2/00427 and by the U.S. National Science Foundation under grant No. PHY-1913028.

## REFERENCES

- [1] C. Fahlander *et al.*, *Nucl. Phys. A* **485**, 327 (1988).
- [2] R.A. Meyer, L. Peker, *Z. Phys. A* **283**, 379 (1977).
- [3] M. Kadi *et al.*, *Phys. Rev. C* **68**, 031306(R) (2003).
- [4] P.E. Garrett *et al.*, *Phys. Rev. C* **75**, 054310 (2007).
- [5] D. Bandyopadhyay *et al.*, *Phys. Rev. C* **76**, 054308 (2007).
- [6] P.E. Garrett *et al.*, *Phys. Rev. C* **86**, 044304 (2012).
- [7] J.C. Batchelder *et al.*, *Phys. Rev. C* **80**, 054318 (2009).
- [8] A.E. Stuchbery, S.K. Chamoli, T. Kibedi, *Phys. Rev. C* **93**, 031302 (2016).

- [9] P.E. Garrett, J.L. Wood, S.W. Yates, *Phys. Scr.* **93**, 063001 (2018).
- [10] P.E. Garrett, J. L. Wood, *J. Phys. G: Nucl. Part. Phys.* **37**, 069701 (2010) [Corrigendum *ibid.* **37**, 069701 (2010)].
- [11] P.E. Garrett *et al.*, *Phys. Rev. Lett.* **123**, 142502 (2019).
- [12] P.E. Garrett *et al.*, to be published in *Phys. Rev. C*, 2020.
- [13] M.T. Esat *et al.*, *Nucl. Phys. A* **274**, 237 (1976).
- [14] Z. Berant *et al.*, *Nucl. Phys. A* **196**, 312 (1972).
- [15] J. Mierzejewski *et al.*, *Nucl. Instrum. Methods Phys. Res. A* **659**, 84 (2011).
- [16] M.B. Würkner *et al.*, *Nucl. Phys. A* **725**, 3 (2003).
- [17] M. Würkner *et al.*, *Acta Phys. Pol. B* **28**, 97 (1997).
- [18] G. Guerdal, F.G. Kondev, *Nucl. Data Sheets* **113**, 1315 (2012).
- [19] K. Kumar, *Phys. Rev. Lett.* **28**, 249 (1972).
- [20] D. Cline, *Annu. Rev. Nucl. Part. Sci.* **36**, 683 (1986).
- [21] K. Hadyńska-Kleń *et al.*, *Phys. Rev. Lett.* **117**, 062501 (2016).
- [22] E. Clément *et al.*, *Phys. Rev. Lett.* **116**, 022701 (2016).
- [23] K. Wrzosek-Lipska *et al.*, *Phys. Rev. C* **86**, 064305 (2012).
- [24] A. Leviatan, N. Gavrielov, J.E. García-Ramos, P. Van Isacker, *Phys. Rev. C* **98**, 031302(R) (2018).
- [25] K. Nomura, J. Jolie, *Phys. Rev. C* **98**, 024303 (2018).
- [26] L. Próchniak, P. Quentin, M. Imadalou, *Int. J. Mod. Phys. E* **21**, 1250036 (2012).
- [27] L. Próchniak, S.G. Rohoziński, *J. Phys. G: Nucl. Part. Phys.* **36**, 123101 (2009).
- [28] L. Próchniak, *Phys. Scr.* **90**, 114005 (2015).
- [29] M. Zielińska *et al.*, *Eur. Phys. J. A* **52**, 99 (2016).
- [30] T. Czosnyka, D. Cline, C.Y. Wu, *Bull. Amer. Phys. Soc.* **28**, 745 (1983).
- [31] GOSIA User's Manual, <http://slcj.uw.edu.pl/en/gosia-code/>
- [32] M. Rocchini *et al.*, *Phys. Scr.* **92**, 074001 (2017).